J|A|C|S
ARTICLES
Published on Web 02/08/2002

Structural Modulation of Molybdenyl Iodate Architectures by Alkali Metal Cations in $AMoO_3(IO_3)$ (A = K, Rb, Cs): A Facile Route to New Polar Materials with Large SHG Responses

Richard E. Sykora,[†] Kang Min Ok,[‡] P. Shiv Halasyamani,[‡] and Thomas E. Albrecht-Schmitt*[,†]

Contribution from the Departments of Chemistry, Auburn University, Auburn, Alabama 36849, and University of Houston, Houston, Texas 77204-5003

Received September 18, 2001

Abstract: Three new molybdenyl iodates, $KMoO_3(IO_3)$ **(1)**, $RbMoO_3(IO_3)$ **(2)**, and $CsMoO_3(IO_3)$ **(3)**, have been prepared through the hydrothermal reactions of MoO_3 with AIO_4 (A = K, Rb, or Cs) at 180 °C. These compounds are isolated as nearly colorless, air-stable crystals. Single-crystal X-ray diffraction experiments reveal that **1** possesses a corrugated layered structure constructed from molybdenum oxide chains that are bridged by iodate anions. The puckering of the layers is caused by the alignment of bent molybdenyl (MoO_2^{2+}) groups along one side of the molybdenum oxide chains. The K^+ cations separate these layers from one another and serve to balance charge. In contrast, compounds **2** and **3**, which are isostructural, form three-dimensional structures with small cavities filled with Rb^+ or Cs^+ cations. The differences between the structures of **1** and those of **2** and **3** are due to rotation of the molybdenyl units as translation occurs down the molybdenum oxide chains in order to accommodate the increased size of the Rb^+ and Cs^+ cations. This rotation allows for the iodate anions to bridge the molybdenum oxide chains in an additional dimension, creating a three-dimensional network structure. Furthermore, while **1** crystallizes in a centrosymmetric space group, **2** and **3** crystallize in polar space groups. Second-harmonic generation measurements on **2** and **3** show large responses of 400× α-quartz. Differential scanning calorimetry measurements demonstrate that **2** and **3** are thermally stable to 494 and 486 °C, respectively. UV−vis diffuse reflectance spectra of these compounds show a high degree of transparency from 1 to 3 eV and a band gap of 3.1 eV.

Introduction

The successful preparation of new nonlinear optical (NLO), piezoelectric, and ferroelectric materials is dictated by the ability to control structure at both the molecular and higher-dimensional levels. To accomplish this goal, structural building units that impart asymmetry must be incorporated into the architecture of the compound to create a noncentrosymmetric (NCS) structure.[1−3] In this regard, several independent approaches have been developed, including the supramolecular engineering of inorganic−organic hybrids,[4−6] the preparation of phases with cooperative second-order Jahn−Teller distortions (SOJT),[7−10] and the design of multilayered films of aligned polar organic molecules.[11−13] Each of these routes has yielded materials with large second-harmonic-generation (SHG) responses, and compounds such as bis(nicotinato)zinc,[4] whose SHG response is 1000× that of α-quartz, clearly demonstrate the tremendous possibilities for further advances in the preparation of new NLO materials.

An alternative method for synthesizing acentric materials is to incorporate pyramidal ligands with a nonbonding, but stereochemically active, pair of electrons, such as selenite[14−16] or iodate,[17−26] into crystalline solids. These anions have a

[†] Auburn University.
[‡] University of Houston.

(1) Hahn, T. *International Tables for Crystallography*; D. Reidel Publishing Co.: Dordrecht, 1983.
(2) Glazer, A. M.; Stadnicka, K. *Acta Crystallogr.* **1989**, *A45*, 234.
(3) Halasyamani, P. S.; Poeppelmeier, K. R. *Chem. Mater.* **1998**, *10*, 2753.
(4) Lin, W.; Evans, O. R.; Xiong, R.-G.; Wang, Z. *J. Am. Chem. Soc.* **1998**, *120*, 13272.
(5) Evans, O. R.; Lin, W. *Chem. Mater.* **2001**, *13*, 3009.
(6) Lin, W.; Wang, Z.; Ma, L. *J. Am. Chem. Soc.* **1999**, *121*, 11249.
(7) Halasyamani, P. S.; O'Hare, D. *Chem. Mater.* **1998**, *10*, 646.
(8) Halasyamani, P. S.; O'Hare, D. *Inorg. Chem.* **1997**, *36*, 6409.
(9) Porter, Y.; Bhuvanesh, N. S. P.; Halasyamani, P. S. *Inorg. Chem.* **2001**, *40*, 1172.
(10) Porter, Y.; Ok, K. M.; Bhuvanesh, N. S. P.; Halasyamani, P. S. *Chem. Mater.* **2001**, *13*, 1910.
(11) Lin, W.; Lin, W.; Wong, G. K.; Marks, T. J. *J. Am. Chem. Soc.* **1996**, *118*, 8034.
(12) Lin, W.; Lee, T.-L.; Lyman, P. F.; Lee, J.; Bedzyk, M. J.; Marks, T. J. *J. Am. Chem. Soc.* **1997**, *119*, 2205.
(13) van der Boom, M. E.; Richter, A. G.; Malinsky, J. E.; Lee, P. A.; Armstrong, N. R.; Dutta, P.; Marks, T. J. *Chem. Mater.* **2001**, *12*, 15.
(14) Kwon, Y.-U.; Lee, K.-S.; Kim, Y. H. *Inorg. Chem.* **1996**, *35*, 1161.
(15) Vaughey, J. T.; Harrison, W. T. A.; Dussack, L. L.; Jacobson, A. J. *Inorg. Chem.* **1994**, *33*, 4370.
(16) (a) Harrison, W. T. A.; Dussack, L. L.; Jacobson, A. J. *J. Solid State Chem.* **1996**, *125*, 234. (b) Harrison, W. T. A.; Dussack, L. L.; Jacobson, A. J. *Inorg. Chem.* **1994**, *33*, 6043. (c) Dussack, L. L.; Harrison, W. T. A.; Jacobson, A. J. *Mater. Res. Bull.* **1996**, *31*, 249.
(17) Svenson, C.; Abrahams, S. C.; Bernstein, J. L. *J. Solid State Chem.* **1981**, *36*, 195.
(18) Nassau, K.; Shiever, J. W.; Prescott, B. E. *J. Solid State Chem.* **1973**, *7*, 186.
(19) Nassau, K.; Shiever, J. W.; Prescott, B. E. *J. Solid State Chem.* **1973**, *8*, 260.
(20) Nassau, K.; Shiever, J. W.; Prescott, B. E.; Cooper, A. S. *J. Solid State Chem.* **1974**, *11*, 314.

propensity for undergoing at least partial alignment in the solid state to create NCS structures that are often polar. For instance, the selenite anion has been used to prepare a series of early transition metal compounds including $AVSeO_5$ ($A = Rb^+$, Cs^+),[14] $A(VO)_3(SeO_3)_2$ ($A = NH_4^+$, K^+, Rb^+, or Cs^+),[14,15] and $A_2(MoO_3)_3SeO_3$ ($A = NH_4^+$, Rb^+, Cs^+, or Tl^+).[16] In addition to alignment of the selenite anions in the latter compounds, the MoO_6 polyhedra are actually highly perturbed from idealized octahedral symmetry owing to a second-order Jahn−Teller distortion (SOJT).[27−32] This type of distortion is prevalent in high-valent, d^0 transition metals owing to the symmetry-allowed mixing of a low-lying excited state with a nondegenerate ground-state molecular orbital.[33−35] This orbital mixing results in a significant distortion of the geometry of the metal centers along the C_2, C_3, or C_4 axes that becomes amplified with increasing charge on the metal centers because the gap between the excited state and the ground state undergoes a simultaneous decrease in size.[33−35]

In a similar fashion, the iodate anion has been utilized in transition metal and lanthanide chemistry to prepare compounds that may serve as optoelectronic materials. Again, alignment of the pyramidal anions often occurs in these solids to create NCS structures, but also the metals impart additional electronic properties owing to the presence of unpaired electrons or charge-transfer bands. Examples of compounds that combine these features include $Co(IO_3)_2$,[17] $Cu(IO_3)_2$,[18,19] and $Ln(IO_3)_3{\cdot}nH_2O$ ((Ln = Ce − Lu; $n = 0-6$).[20−26] Even simple alkali metal iodates, such as $LiIO_3$, have become standard materials exploited for laser frequency-doubling applications.[36] Typically these compounds are air-stable, are transparent in regions of interest, and have high laser damage thresholds.

In our laboratory, we have focused on the structural and chemical influences of alkali metals, alkaline-earth metals, and transition metals in the hydrothermal preparation of new uranyl iodate compounds.[37−40] These studies have resulted in a series of low-dimensional compounds such as $A_2[(UO_2)_3(IO_3)_4O_2]$ (A = K,[38] Rb,[40] or Tl[40]) and $AE[(UO_2)_2(IO_3)_2O_2](H_2O)$ (AE = Sr,[40] Ba,[38] or Pb[40]), as well as $Ag_4(UO_2)_4(IO_3)_2(IO_4)_2O_2$,[39] which contains the previously unknown tetraoxoiodate (IO_4^{3-}) anion. Unfortunately, the uranyl (UO_2^{2+}) dication is easily placed upon centers of inversion or higher symmetry owing to its linear geometry, and this inhibits the formation of the acentric structures that are so prevalent in iodate chemistry. In an effort to rationally design asymmetry into these compounds, we have replaced the uranyl dications with isoelectronic molybdenyl (MoO_2^{2+}) dications. Not only is Mo(VI) highly susceptible to SOJT distortions (vide supra), but the bent O═Mo═O bond angle of approximately 104° prevents additional moieties from obtaining an idealized geometry around the Mo(VI) center. Furthermore, hydrothermal synthetic techniques have been shown to be highly amenable to the preparation of new molybdenum-containing compounds.[41−45]

Herein we report the hydrothermal synthesis of a series of alkali metal molybdenyl iodates with the general formula $AMoO_3(IO_3)$ ($A = K^+$, Rb^+, or Cs^+). We will demonstrate that the alkali metal cations have a dramatic influence on the molybdenyl iodate architecture and in fact modulate the crystal structures. Finally, SHG powder measurements reveal that these compounds have large SHG responses that may allow for further technological development.[46]

Experimental Section

Syntheses. MoO_3 (99.95%, Alfa-Aesar), CsCl (99.999%, Alfa-Aesar), Cs_2CO_3 (99%, Alfa-Aesar), Rb_2CO_3 (99%, Alfa-Aesar), H_5IO_6 (98%, Alfa-Aesar), and KIO_4 (99.9%, Fisher) were used as received. $RbIO_4$ and $CsIO_4$ were prepared from the reaction of Rb_2CO_3 or Cs_2CO_3 with H_5IO_6 as reported by de Waal et al.[47] Distilled and Millipore-filtered water with a resistance of 18.2 MΩ was used in all reactions. Reactions were run in Parr 4749 23-mL autoclaves with PTFE liners for 3 d at 180 °C and cooled at a rate of 9 °C/h to 23 °C. The resultant mother liquors were decanted from crystalline products that were subsequently washed with methanol. A Leco Tem-Press 27-mL autoclave filled with 20 mL of water and counter-pressured with 2500 psi of argon was employed for reactions at 420 °C. These reactions were run in sealed quartz or gold ampules. *Extreme care should always be taken when scoring and opening sealed tubes from hydrothermal reactions since these are typically under pressure.* SEM/EDX analyses were performed using a JEOL 840/Link Isis instrument. K and Mo percentages were calibrated against standards. Typical results are within 3% of actual ratios. IR spectra were collected on a Nicolet 5PC FT-IR spectrometer from KBr pellets.

$KMoO_3(IO_3)$ (1). MoO_3 (119 mg, 0.83 mmol) and KIO_4 (381 mg, 1.66 mmol) were loaded in a 23-mL PTFE-lined autoclave. Water (1 mL) was then added to the solids. The product mixture included large clusters of colorless plates and large colorless cubes resting in a colorless liquid. The colorless plates (very pale yellow in bulk) of **1** were easily isolated to afford a yield of 268 mg (90% based on Mo), whereas the colorless cubes were established as KIO_3, based on a unit cell determination. EDX analysis for $KMoO_3(IO_3)$ provided a K:Mo:I ratio of 1:1:1. IR (KBr, cm^{-1}): 931 ($Mo{=}O_{sym}$) (s), 916 ($Mo{=}O_{asym}$) (s), 882 (s), 808 (s), 581 (s), 452 (s), 414 (s).

(21) Liminga, R.; Abrahams, S. C.; Bernstein, J. L. *J. Chem. Phys.* **1975**, *62*, 755.
(22) Nassau, K.; Shiever, J. W.; Prescott, B. E. *J. Solid State Chem.* **1975**, *14*, 122.
(23) Abrahams, S. C.; Bernstein, J. L.; Nassau, K. *J. Solid State Chem.* **1976**, *16*, 173.
(24) Abrahams, S. C.; Bernstein, J. L.; Nassau, K. *J. Solid State Chem.* **1977**, *22*, 243.
(25) Liminga, R.; Abrahams, S. C.; Bernstein, J. L. *J. Chem. Phys.* **1977**, *67*, 1015.
(26) Gupta, P. K. S.; Ammon, H. L.; Abrahams, S. C. *Acta Crystallogr.* **1989**, *C45*, 175.
(27) Opik, U.; Pryce, M. H. L. *Proc. R. Soc. London* **1937**, *A161*, 220.
(28) Wheeler, R. A.; Whangbo, M. H.; Hughbanks, T.; Hoffman, R.; Burdett, J. K.; Albright, T. A. *J. Am. Chem. Soc.* **1986**, *108*, 2222.
(29) Pearson, R. G. *J. Mol. Struct.* **1983**, *103*, 25.
(30) Kang, S. K.; Tang, H.; Albright, T. A. *J. Am. Chem. Soc.* **1993**, *115*, 1971.
(31) Cohen, R. E. *Nature* **1992**, *358*, 136.
(32) Burdett, J. K. *Molecular Shapes*; Wiley-Interscience: New York, 1980.
(33) Kunz, M.; Brown, I. D. *J. Solid State Chem.* **1995**, *115*, 395.
(34) Goodenough, J. B.; Longo, J. M. Crystallographic and magnetic properties of perovskite and perovskite-related compounds. In *Landolt-Bornstein*; Hellwege, K. H., Hellwege, A. M., Eds.; Springer-Verlag: Berlin, 1970; Vol. 4, pp 126−314.
(35) Brown, I. D. *Acta Crystallogr.* **1977**, *B33*, 1305.
(36) Rosker, M. J.; Marcy, H. O. New nonlinear materials for high-power frequency conversion: from the near-ultraviolet to the long-wave infrared. In *Novel Optical Materials and Applications*; Khoo, I.-C., Simoni, F., Umeton, C., Eds.; John Wiley & Sons: New York, 1997; pp 175−204.
(37) Bean, A. C.; Peper, S. M.; Albrecht-Schmitt, T. E. *Chem. Mater.* **2001**, *13*, 1266.
(38) Bean, A. C.; Ruf, M.; Albrecht-Schmitt, T. E. *Inorg. Chem.* **2001**, *40*, 3959.
(39) Bean, A. C.; Campana, C. F.; Kwon, O.; Albrecht-Schmitt, T. E. *J. Am. Chem. Soc.* **2001**, *123*, 8806.
(40) Bean, A. C.; Albrecht-Schmitt, T. E. *J. Solid State Chem.* **2001**, *161*, 416.
(41) Finn, R. C.; Zubieta, J. *Inorg. Chem.* **2001**, *40*, 2466.
(42) Hagrman, P. J.; LaDuca, R. L., Jr.; Koo, H.-J.; Rarig, R., Jr.; Haushalter, R. C.; Whangbo, M.-H.; Zubieta, J. *Inorg. Chem.* **2000**, *39*, 4311.
(43) Zapf, P. J.; Hammond, R. P.; Haushalter, R. C.; Zubieta, J. *Chem. Mater.* **1998**, *10*, 1366.
(44) Zapf, P. J.; LaDuca, R. L., Jr.; Rarig, R. S., Jr.; Johnson, K. M., III; Zubieta, J. *Inorg. Chem.* **1998**, *37*, 3411.
(45) Zapf, P. J.; Haushalter, R. C.; Zubieta, J. *Chem. Mater.* **1997**, *9*, 2019.
(46) Sykora, R. E.; Albrecht-Schmitt, T. E. Provisional Patent No. 60/324,136, 2001.
(47) de Waal, D.; Range, K.-J. *Z. Naturforsch.* **1996**, *51b*, 1365.

$RbMoO_3(IO_3)$ (2). MoO_3 (103 mg, 0.72 mmol) and $RbIO_4$ (397 mg, 1.44 mmol) were loaded in a 23-mL PTFE-lined autoclave. Water (1 mL) was then added to the solids. The product mixture consisted of an almost clear and colorless liquid over clusters of colorless plates, along with large colorless cubes. Manual separation of the colorless plates (very pale yellow in bulk) of **2** resulted in the isolation of 261 mg (90% yield based on Mo), while the colorless cubes were determined to be $RbIO_3$. EDX analysis for $RbMoO_3(IO_3)$ provided a Rb:Mo:I ratio of 1:1:1. IR (KBr, cm^{-1}): 935 ($Mo{=}O_{sym}$) (m), 882 (s), 861 (s), 812 (s), 789 (s), 766 (m), 740 (s, sh), 721 (s), 670 (s, br), 448 (w), 420 (m).

$CsMoO_3(IO_3)$ (3). MoO_3 (91 mg, 0.63 mmol) and $CsIO_4$ (409 mg, 1.26 mmol) were loaded in a 23-mL PTFE-lined autoclave. Water (3 mL) was then added to the solids. The product mixture consisted of an almost clear and colorless liquid over clusters of very pale yellow rods, along with large colorless cubes. Manual separation of the very pale yellow rods of **3** produced 237 mg (83% yield based on Mo), while the colorless cubes were determined to be $CsIO_3$. EDX analysis for $CsMoO_3(IO_3)$ provided a Cs:Mo:I ratio of 1:1:1. IR (KBr, cm^{-1}): 938 ($Mo{=}O_{sym}$) (m), 878 (s), 857 (s), 814 (s), 797 (s), 768 (s), 743 (s), 709 (s), 668 (s, br), 441(w), 418 (m).

Thermal Analysis. Thermal data for compounds **1**−**3** were collected using a TA Instruments model 2920 differential scanning calorimeter (DSC). Samples (∼15 mg) were encapsulated in aluminum pans and heated at 10 °C/min from 25 to 600 °C under a nitrogen atmosphere.

Secord-Order NLO Measurements. Powder SHG measurements were performed on a modified Kurtz-NLO system using a 1064-nm light source.[48] A detailed description of the apparatus has been published.[10] Polycrystalline $RbMoO_3(IO_3)$ and $CsMoO_3(IO_3)$ were ground separately and sieved into distinct particle size ranges, <20, 20−45, 45−63, 63−75, 75−90, and 90−125 μm. To make relevant comparisons with known SHG materials, crystalline SiO_2 and $LiNbO_3$ were also ground and sieved into the same particle size range. All of the powders were placed in separate capillary tubes. No index-matching fluid was used in any of the experiments. $I^{2\omega}/I^{2\omega}(SiO_2)$ is taken for a particle size range of 45−63 μm.

UV−Vis Diffuse Reflectance Spectra. Diffuse reflectance spectra for **2** and **3** were measured from 1800 to 200 nm using a Shimadzu UV3100 spectrophotometer equipped with an integrating sphere attachment, with $BaSO_4$ being used as the standard. The Kubelka−Monk function was used to convert diffuse reflectance data to absorbance spectra.[49]

Crystallographic Studies. Single crystals of **1**, **2**, and **3** with the dimensions 0.032 mm × 0.140 mm × 0.140 mm, 0.040 mm × 0.080 mm × 0.080 mm, and 0.046 mm × 0.046 mm × 0.196 mm, respectively, were mounted on glass fibers and aligned on a Bruker SMART APEX CCD X-ray diffractometer. For each crystal, intensity measurements were performed using graphite-monochromated Mo Kα radiation from a sealed tube and a monocapillary collimator. SMART was used for preliminary determination of the cell constants and data collection control. The intensities of reflections of a sphere were collected by a combination of three sets of exposures (frames). Each set had a different ϕ angle for the crystal, and each exposure covered a range of 0.3° in ω. A total of 1800 frames were collected with an exposure time per frame of 30 s.

The determination of integral intensities and global cell refinement were performed with the Bruker SAINT (v 6.02) software package using a narrow-frame integration algorithm. A semiempirical absorption correction was applied, based on the intensities of symmetry-related reflections measured at different angular settings using SADABS.[50] The program suite SHELXTL (v 5.1) was used for space group determination (XPREP), structure solution (XS), and refinement (XL).[51] The final refinement included anisotropic displacement parameters for all atoms. Some crystallographic details are listed in Table 1; additional details can be found in the Supporting Information.

Table 1. Crystallographic Data for $KMoO_3(IO_3)$ (**1**), $RbMoO_3(IO_3)$ (**2**), and $CsMoO_3(IO_3)$ (**3**)

formula	$KMoO_3(IO_3)$	$RbMoO_3(IO_3)$	$CsMoO_3(IO_3)$
formula mass (amu)	357.94	404.31	451.75
space group	*Pbca* (No. 61)	$Pna2_1$ (No. 33)	$Pna2_1$ (No. 33)
a (Å)	7.7991(3)	7.7277(6)	7.8633(5)
b (Å)	7.3372(3)	10.2137(8)	10.3920(6)
c (Å)	19.2695(8)	7.3442(6)	7.3869(5)
V (Å^3)	1102.67(8)	579.67(8)	603.62(7)
Z	8	4	4
T (°C)	−80	−80	−80
λ (Å)	0.71073	0.71073	0.71073
ρ_{calcd} (g cm^{-3})	4.312	4.633	4.971
μ(Mo Kα) (cm^{-1})	86.88	158.88	131.90
$R(F)$ for $F_o^2 > 2\sigma(F_o^2)$[a]	0.0216	0.0194	0.0209
$R_w(F_o^2)$[b]	0.0525	0.0421	0.0517

[a] $R(F) = \sum||F_o| - |F_c||/\sum|F_o|$. [b] $R_w(F_o^2) = [\sum[w(F_o^2 - F_c^2)^2]/\sum wF_o^4]^{1/2}$.

Results and Discussion

Syntheses. The reactions of MoO_3 with KIO_4, $RbIO_4$, or $CsIO_4$ under mild hydrothermal conditions results in the formation of $KMoO_3(IO_3)$ (**1**), $RbMoO_3(IO_3)$ (**2**), or $CsMoO_3(IO_3)$ (**3**), respectively. These compounds are produced as moderate-sized, nearly colorless crystals. While AIO_3 ($A = K^+$, Rb^+, Cs^+) are also isolated as byproducts from these reactions, an excess of AIO_4 improves both the yield and crystal quality of **1**−**3**. In addition, we have found that these reactions are cation selective in that the reaction of MoO_3 with KIO_4 and CsCl only produces **3**. We have been unable to prepare **1**−**3** by using I_2O_5 or HIO_3 as the source of iodate. This is a consequence of pH dependence on product formation since the change of I_2O_5 to AIO_4 ($A = K^+$, Rb^+, Cs^+) starting materials results in a dramatic increase in pH. The pH of the reaction described for the synthesis of **3** is 3.9. When CsCl and I_2O_5 are substituted for $CsIO_4$, the pH is lowered to 0.3. The observed reduction of heptavalent iodine in the metaperiodate, IO_4^-, starting materials to pentavalent iodine in IO_3^- is a ubiquitous reaction in our hydrothermal chemistry that we have also noted in the syntheses of uranyl iodate compounds.[37−40,52] We propose that water is the reducing agent in these reactions.

Explorations of crystal growth conditions have shown that the crystal sizes of **2** and **3** are related to the amount of water employed in the reactions with crystals of larger size growing from larger volumes of water. For instance, crystals of **3** several millimeters in length can be grown by reacting MoO_3 (1.26 mmol) with $CsIO_4$ (2.53 mmol) in 10 mL of water at 180 °C for 3 days. Furthermore, the synthesis of **3** can easily be scaled up to produce gram quantities of these crystals.

Structures. The structures of compounds **1**−**3** are all constructed from nearly identical six-coordinate *cis*-$MoO_4(IO_3)_2$ fundamental building units, as shown in Figure 1. These units corner-share two *trans* oxygen atoms with neighboring polyhedra to form an infinite one-dimensional molybdenum oxide chain. These chains are then bridged by the iodate anions. The key difference between the structure of **1** and those of **2** and **3**

(48) Kurtz, S. K.; Perry, T. T. *J. Appl. Phys.* **1968**, *39*, 3798.
(49) Wendlandt, W. W.; Hecht, H. G. *Reflectance Spectroscopy*; Interscience Publishers: New York, 1966.
(50) *SADABS*, Program for absorption correction using SMART CCD based on the method of Blessing: Blessing, R. H. *Acta Crystallogr.* **1995**, *A51*, 33.
(51) Sheldrick, G. M. SHELXTL PC, Version 5.0, An Integrated System for Solving, Refining, and Displaying Crystal Structures from Diffraction Data; Siemens Analytical X-ray Instruments, Inc.: Madison, WI, 1994.

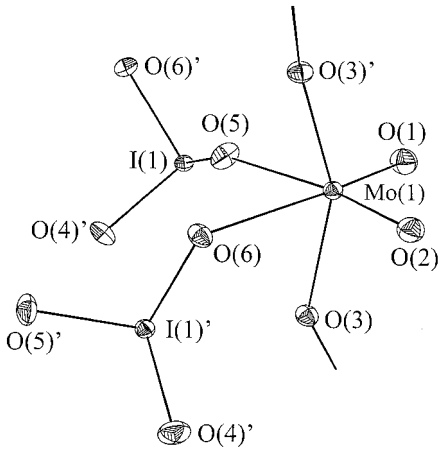

Figure 1. View of the six-coordinate *cis*-$MoO_4(IO_3)_2$ structural building units in $KMoO_3(IO_3)$ (**1**), $RbMoO_3(IO_3)$ (**2**), and $CsMoO_3(IO_3)$ (**3**). The Mo(VI) centers show orthorhombic distortions along a C_2 axis of an idealized octahedron owing to a second-order Jahn−Teller distortion; 50% probability ellipsoids are shown for **1**.

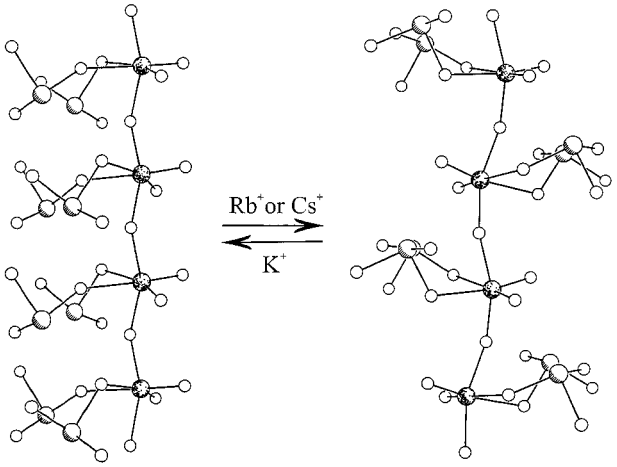

Figure 2. Depiction of the differences between one-dimensional molybdenum oxide chains built from *cis*-$MoO_4(IO_3)_2$ units in the structure of $KMoO_3(IO_3)$ (**1**) versus those observed for $RbMoO_3(IO_3)$ (**2**) and $CsMoO_3(IO_3)$ (**3**). In **2** and **3**, a 2_1 rotation occurs down the polar *c*-axis, whereas the molybdenyl (MoO_2^{2+}) units align on one side of the chain in $KMoO_3(IO_3)$.

(the latter two being isostructural) is that as translation occurs down the molybdenum oxide chains, the molybdenyl (MoO_2^{2+}) units align on one side of the chain in **1**, whereas in **2** and **3** the *cis*-$MoO_4(IO_3)_2$ units are subject to a 2_1 rotation down the polar *c*-axis, as illustrated in Figure 2. In **1**, the alignment of the molybdenyl units creates a corrugated layered structure, as shown in Figure 3. In contrast, the rotation of the *cis*-$MoO_4(IO_3)_2$ units in **2** and **3** connects alternating molybdenum centers on all sides of the chains, creating a three-dimensional solid, as depicted in Figure 4. In compounds **1**−**3**, the alkali metal cations serve to fill the void spaces and to balance charge. In **1**, the K^+ cations reside in eight-coordinate square antiprismatic environments, while in **2** and **3**, the Rb^+ and Cs^+ cations possess nine-coordinate distorted geometries. These cations, however, clearly play an additional role in that the increase in ionic radii from K^+ (1.65 Å) to Rb^+ (1.75 Å) or Cs^+ (1.90 Å) is the source of the substantial structural transformation observed between **1** and **2** or **3**.[53] Furthermore, it has been noted by Bergman et al.

(52) Gorski, A.; Milczarek, M. *Pol. J. Chem.* **1984**, *58*, 635.

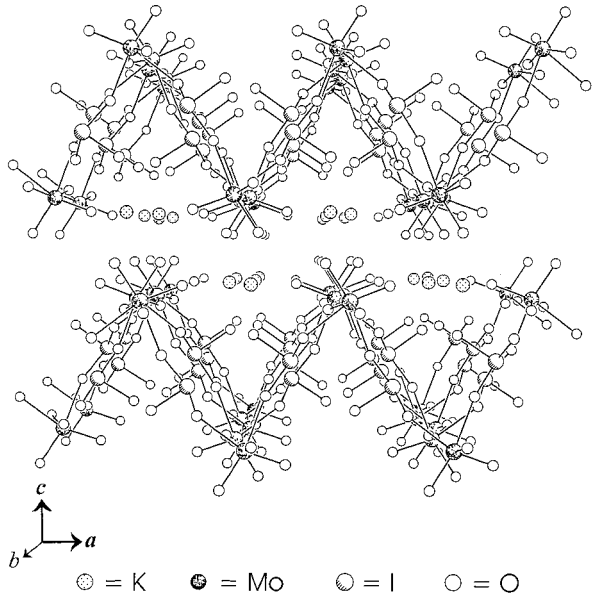

Figure 3. Illustration of the corrugated layered structure of $KMoO_3(IO_3)$ (**1**) created by the alignment of the molybdenyl (MoO_2^{2+}) units. The K^+ cations serve to separate the $^2_\infty[MoO_3(IO_3)]^-$ layers from one another and to balance charge.

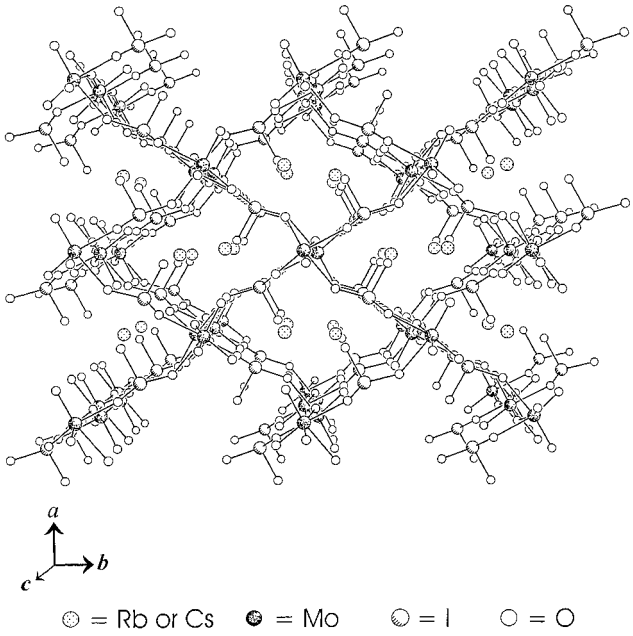

Figure 4. Three-dimensional structures of $RbMoO_3(IO_3)$ (**2**) and $CsMoO_3(IO_3)$ (**3**) created by the bridging of molybdenum oxide chains by iodate anions. The small cavities in this structure are occupied by the Rb^+ or Cs^+ cations. As these compounds are isostructural, only part of the structure of $CsMoO_3(IO_3)$ is shown.

that large cations such as Cs^+ and Ba^{2+} have a tendency to adopt acentric coordination environments, aiding in the formation of NCS compounds.[54]

The Mo(VI) centers in the *cis*-$MoO_4(IO_3)_2$ polyhedra are highly distorted from idealized octahedral symmetry, as shown in Figure 1. Based on an average of the bond lengths in the structures of **1**−**3**, these hexavalent cations display a 2 + 2 + 2 bonding scheme, with two long bonds of 2.243(4) Å, two

(53) Shannon, R. D. *Acta Crystallogr.* **1976**, *A32*, 751.
(54) Bergman, J. G., Jr.; Boyd, G. D.; Ashkin, A.; Kurtz, S. K. *J. Appl. Phys.* **1969**, *70*, 2860.

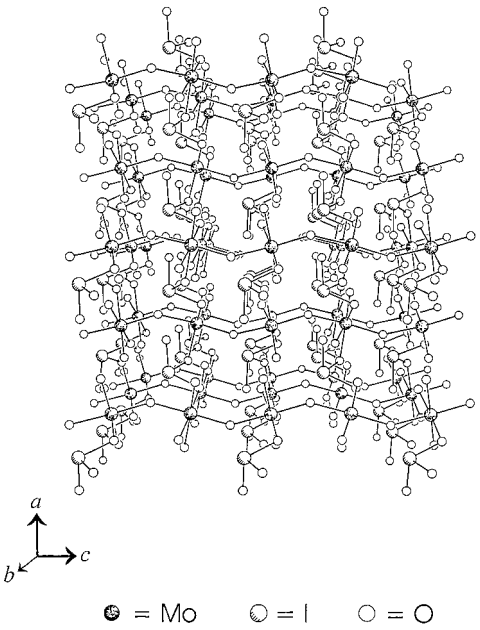

Figure 5. View down the *b*-axis showing the alignment of the stereochemically active lone pairs of electrons on the iodate anions that gives rise to part of the polarity in the structures of $RbMoO_3(IO_3)$ (**2**) and $CsMoO_3(IO_3)$ (**3**). These anions are aligned along the polar *c*-axis. Rb^+ or Cs^+ cations have been omitted for clarity.

intermediate bonds of 1.945(4) Å, and two short bonds of 1.716(4) Å. The two short distances result from the Mo═O double bonds that define the molybdenyl (MoO_2^{2+}) unit, the intermediate distances are the bonds to the bridging oxo groups, and the two longest bonds are those with the oxygen atoms from the bridging iodate ligands. This bonding pattern is readily explained by an orthorhombic, second-order Jahn−Teller distortion along a C_2 axis of the MoO_6 octahedron.[33,34] As previously discussed, the Mo(VI) centers are readily susceptible to such distortions, because while the ground state (HOMO) has octahedral symmetry, there is a low-lying excited state (LUMO) close enough in energy to allow for mixing. This results in a lowering of symmetry of the Mo(VI) center.[33,34] Furthermore, because the HOMO−LUMO gap decreases in size with increasing charge on the metal center, metal ions capable of obtaining high oxidation states, such as Mo(VI), tend to show particularly pronounced distortions.[3,33,34] This type of distortion has also been noted in other Mo(VI) compounds, including Mo(VI) selenites.[14−16] Bond valence sum calculations help to further illustrate the high valency of the Mo centers, with values of 6.01, 5.95, and 6.04 being determined for **1**, **2**, and **3**, respectively.[55,56]

The final important feature in the structures of **1**−**3** is the orientation of the C_{3v} iodate anions or, more specifically, the alignment of the stereochemically active lone pair of electrons on the iodine atoms. Compound **1** crystallizes in the centrosymmetric space group *Pbca*, whose origin is at $\bar{1}$. This precludes any possibility of net alignment of either the iodate anions or the SOJT distortion of the Mo(VI) centers. Compounds **2** and **3**, however, crystallize in the polar space group $Pna2_1$, which is in the crystal class *mm*2. Therefore, the polarity in the structures should be along the *c*-axis. Examinations of the crystal structure show that the iodate groups do indeed display net alignment along the polar *c*-axis, as illustrated in Figure 5. Selected bond distances and angles for **1**, **2**, and **3** are given in Tables 2, 3, and 4, respectively.

Table 2. Selected Bond Distances (Å) and Angles (Deg) for $KMoO_3(IO_3)$ (**1**)

		Distances	
Mo(1)−O(1)	1.710(2)	Mo(1)−O(2)	1.719(2)
Mo(1)−O(3)	2.020(2)	Mo(1)−O(3)′	1.897(2)
Mo(1)−O(5)	2.186(2)	Mo(1)−O(6)′	2.236(2)
I(1)−O(4)	1.779(2)	I(1)−O(5)	1.820(2)
I(1)−O(6)	1.845(2)		
		Angles	
O(1)−Mo(1)−O(2)	103.4(1)	O(1)−Mo(1)−O(3)′	103.1(1)
O(2)−Mo(1)−O(3)′	97.3(1)	O(1)−Mo(1)−O(3)	97.0(1)
O(2)−Mo(1)−O(3)	93.6(1)	O(3)′−Mo(1)−O(3)	154.2(1)
O(1)−Mo(1)−O(5)	88.6(1)	O(2)−Mo(1)−O(5)	168.0(1)
O(3)′−Mo(1)−O(5)	80.95(9)	O(3)−Mo(1)−O(5)	83.56(9)
O(1)−Mo(1)−O(6)′	161.7(1)	O(2)−Mo(1)−O(6)′	93.7(1)
O(3)′−Mo(1)−O(6)′	81.00(9)	O(3)−Mo(1)−O(6)′	75.00(9)
O(5)−Mo(1)−O(6)′	74.31(9)		

Table 3. Selected Bond Distances (Å) and Angles (Deg) for $RbMoO_3(IO_3)$ (**2**)

		Distances	
Mo(1)−O(1)′	1.712(4)	Mo(1)−O(2)	1.727(4)
Mo(1)−O(3)′	1.894(4)	Mo(1)−O(3)	1.987(4)
Mo(1)−O(5)	2.216(4)	Mo(1)−O(6)′	2.285(3)
I(1)−O(4)	1.811(3)	I(1)−O(5)	1.832(3)
I(1)−O(6)	1.815(3)		
		Angles	
O(1)′−Mo(1)−O(2)	104.0(2)	O(1)′−Mo(1)−O(3)′	96.8(2)
O(2)−Mo(1)−O(3)′	98.0(2)	O(1)′−Mo(1)−O(3)	94.8(2)
O(2)−Mo(1)−O(3)	93.6(2)	O(3)′−Mo(1)−O(3)	161.14(3)
O(1)′−Mo(1)−O(5)	165.0(2)	O(2)−Mo(1)−O(5)	89.8(2)
O(3)′−Mo(1)−O(5)	87.0(1)	O(3)−Mo(1)−O(5)	78.2(1)
O(1)′−Mo(1)−O(6)′	86.6(2)	O(2)−Mo(1)−O(6)′	168.9(2)
O(3)′−Mo(1)−O(6)′	83.9(2)	O(3)−Mo(1)−O(6)′	82.0(2)
O(5)−Mo(1)−O(6)′	79.4(1)		

Nonlinear Optical Properties. Given the *mm*2 crystal class of **2** and **3**, we thought it was important to provide independent verification of their acentric space group and to measure the SHG responses of these compounds. SHG measurements were performed using a modified Kurtz-NLO system with a 1064-nm light source on powders ground from crystals of **2** and **3**. Generation of SHG light of 532 nm was carefully measured, and these studies indicated large responses for **2** and **3** of 400× α-quartz. The materials are also phase-matchable, as shown in Figures 6 and 7. Calculations using methods described earlier[10,57] give an average NLO susceptibility, $\langle d_{ijk}^{2\omega} \rangle$ or $\langle d_{\text{eff}} \rangle$, of 23 pm/V. The large responses of **2** and **3** are due not only to the polarity of the space group and the alignment of the lone pairs on the iodate anions, but also to the large degree of polarization of the Mo−O bonds.

Thermal Behavior. To evaluate the thermal behavior of **1**−**3**, DSC thermograms were measured from 25 to 600 °C under a flowing nitrogen atmosphere. It is well established that iodate compounds decompose through thermal disproportionation to yield metaperiodates or periodates, oxygen, and iodine.[52] Compounds **2** and **3** show simple thermograms, with the onset of endothermic decomposition occurring at 494 and 486 °C,

(55) Brown, I. D.; Altermatt, D. *Acta Crystallogr.* **1985**, *B41*, 244.
(56) Brese, N. E.; O'Keeffe, M. *Acta Crystallogr.* **1991**, *B47*, 192.
(57) Ok, K. M.; Bhuvanesh, N. S. P.; Halasyamani, P. S. *J. Solid State Chem.* **2001**, *161*, 57.

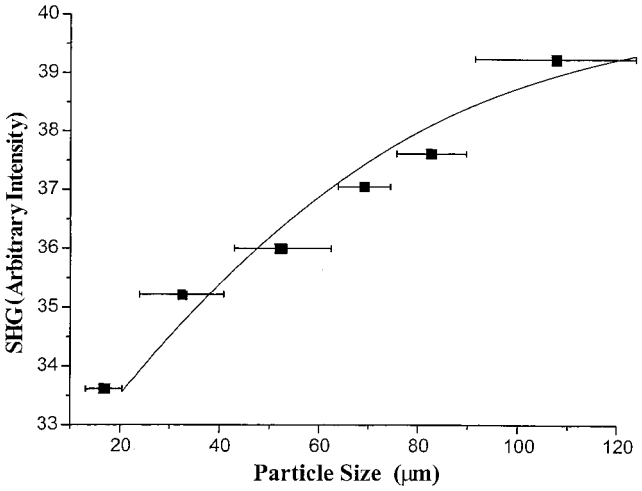

Figure 6. Phase matching curve (particle size) vs SHG intensity for $RbMoO_3(IO_3)$ (**2**).

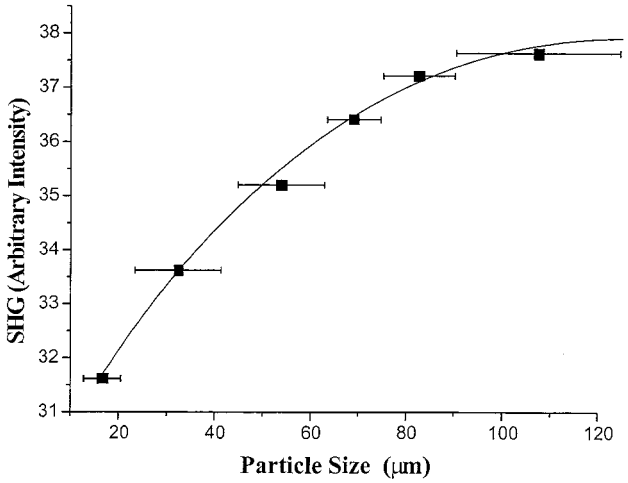

Figure 7. Phase matching curve (particle size) vs SHG intensity for $CsMoO_3(IO_3)$ (**3**).

Table 4. Selected Bond Distances (Å) and Angles (Deg) for $CsMoO_3(IO_3)$ (**3**)

Distances			
Mo(1)−O(1)′	1.710(4)	Mo(1)−O(2)	1.715(4)
Mo(1)−O(3)′	1.856(4)	Mo(1)−O(3)	2.015(4)
Mo(1)−O(5)	2.207(4)	Mo(1)−O(6)′	2.330(4)
I(1)−O(4)	1.798(4)	I(1)−O(5)	1.835(4)
I(1)−O(6)	1.808(4)		
Angles			
O(1)′−Mo(1)−O(2)	103.0(2)	O(1)′−Mo(1)−O(3)′	97.2(2)
O(2)−Mo(1)−O(3)′	98.5(2)	O(1)′−Mo(1)−O(3)	92.8(2)
O(2)−Mo(1)−O(3)	93.5(2)	O(3)′−Mo(1)−O(3)	162.20(3)
O(1)′−Mo(1)−O(5)	163.9(2)	O(2)−Mo(1)−O(5)	91.4(2)
O(3)′−Mo(1)−O(5)	87.6(2)	O(3)−Mo(1)−O(5)	79.0(2)
O(1)′−Mo(1)−O(6)′	85.5(2)	O(2)−Mo(1)−O(6)′	170.7(2)
O(3)′−Mo(1)−O(6)′	83.8(2)	O(3)−Mo(1)−O(6)′	82.3(2)
O(5)−Mo(1)−O(6)′	79.7(1)		

respectively. This decomposition is in the same temperature range as those of other iodate compounds that we and others have investigated.[20,22] These peaks are linked to exotherms at 501 and 489 °C for **2** and **3**, respectively. These exotherms correspond to reactions with the aluminum pans, resulting in the formation of $MAl(MoO_4)_2$ ($M = Rb^+, Cs^+$), as established by single-crystal X-ray diffraction.[58]

The thermal behavior of **1** is similar to that of **2** and **3** in that thermal disproportionation occurs at 453 °C. However, an additional broadened endotherm centered around 404 °C is also observed. We became suspicious that this transformation actually corresponds to a phase transition of **1** to the same structure type as that of **2** and **3**. Therefore, we investigated several hydrothermal reactions of MoO_3 with KIO_4 at 420 °C for 3 days. This reaction temperature is higher than the observed endotherm at 404 °C and should therefore allow for the observation of any transformations of **1**. Under these conditions, only **1** and elemental iodine were isolated as solids. The observation of iodine as a product of these reactions can be ascribed to the high temperatures that cause thermal disproportionation of iodate. Unfortunately, there is only a narrow window of approximately 50 °C between the endotherm at 404 °C and thermal disproportionation at 453 °C, preventing higher temperature reactions from revealing any possible phase transformations.

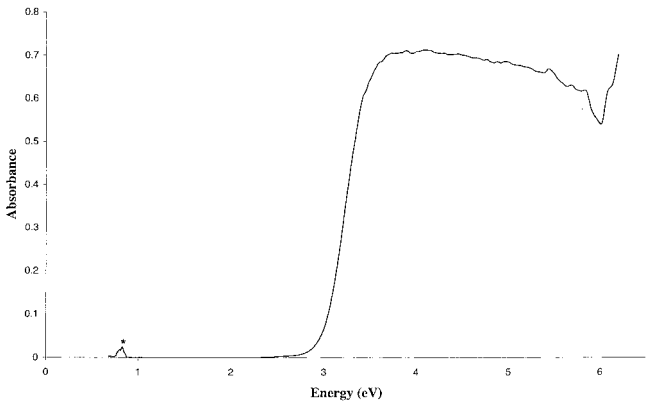

Figure 8. UV−vis diffuse reflectance spectrum of $CsMoO_3(IO_3)$ (**3**) showing the absorption edge at 3.1 eV. Instrument artifact is denoted by ∗.

UV−Vis Diffuse Reflectance Spectra. The transparency of potential NLO materials in regions of interest is of critical concern since minimal absorbance of the source and SHG light reduces laser damage to the crystal and improves efficiency. Furthermore, the electronic spectra of these compounds provide fundamental information on the nature of conduction in these extended structures. UV−vis diffuse reflectance spectra were collected from crystalline samples that were ground into fine powders. The spectrum of **3** from 1800 to 200 nm is shown (in electronvolts) in Figure 8. The spectrum of **2** is nearly identical to that of **3** and is not shown for the sake of brevity. These spectra show that **2** and **3** are essentially transparent to approximately 3 eV. Plots of absorbance squared versus energy and the square root of absorbance versus energy at the absorption edge (3−3.4 eV) both show nearly linear dependence, with R^2 values of 0.9745 and 0.9911, respectively. Therefore, it is unclear whether these compounds have direct or indirect band gaps. Extrapolation of absorbance squared versus energy to absorbance = 0 provides an approximate band gap of 3.10 eV.[59,60]

Conclusions

In this study we have demonstrated that new polar materials with large SHG responses can be created by combining

(58) Klevtsova, R. F.; Klevtsova, P. V. *Kristallographia* **1970**, *15*, 953.
(59) Pankove, J. I. *Optical Processes in Semiconductors*; Prentice Hall, Inc.: Engelwood Cliffs, NJ, 1971.
(60) Feger, C. R.; Kolis, J. W.; Gorny, K.; Pennington, C. *J. Solid State Chem.* **1999**, *143*, 254.

transition metals with highly asymmetric coordination environments, such as Mo(VI) in the form of molybdenyl, with anions containing a stereochemically active lone pair of electrons. These high-valent metals have the additional benefit of polarizing M−O bonds, which aids in obtaining a substantial SHG response. These compounds are thermally robust and show good transparency from 1 to 3 eV. In future studies, we will address the use of additional countercations in these hydrothermal syntheses so as to ascertain their role in the formation of these new inorganic architectures.

Acknowledgment. T.E.A.-S. acknowledges NASA (ASGC) and the Department of Energy, Heavy Elements Program (Grant No. DE-FG02-01ER15187), for partial support of this work. P.S.H. acknowledges the Robert A. Welch Foundation for support. This work used the MRSEC/TCSUH Shared Experimental Facilities supported by the National Science Foundation under Award No. DMR-9632667 and the Texas Center for Superconductivity at the University of Houston. This work was also supported by the NSF-Career Program through DMR-0092054, and an acknowledgment is made to the donors of the Petroleum Research Fund, administered by the American Chemical Society, for partial support of this research. The authors also thank Mutlu Kartin (Clemson University) for assistance in obtaining the UV−vis diffuse reflectance spectra.

Supporting Information Available: X-ray crystallographic files for **1**−**3** (CIF). This material is available free of charge via the Internet at http://pubs.acs.org.

JA012190Z